







# Delineation of the GPR15 receptor-mediated G $\alpha$ protein signalling profile in recombinant mammalian cells

Yufang Deng<sup>1</sup>  | Ee Von Moo<sup>1</sup>  | Claudia Victoria Pérez Almería<sup>1,2</sup>  |  
 Patrick R. Gentry<sup>1,3</sup>  | Line Vedel<sup>1,3</sup> | Jesper M. Mathiesen<sup>1</sup>  |  
 Hans Bräuner-Osborne<sup>1</sup> 

<sup>1</sup>Department of Drug Design and Pharmacology, Faculty of Health and Medical Sciences, University of Copenhagen, Copenhagen

<sup>2</sup>Amsterdam Institute for Molecular and Life Sciences (AIMMS), Division of Medicinal Chemistry, Faculty of Science, Vrije Universiteit Amsterdam, Amsterdam, The Netherlands

<sup>3</sup>Analytical Technology Department, FUJIFILM Diosynth Biotechnologies, Hillerød, Denmark

## Correspondence

Hans Bräuner-Osborne, Department of Drug Design and Pharmacology, Faculty of Health and Medical Sciences, University of Copenhagen, Copenhagen, Denmark.

Email: [hbo@sund.ku.dk](mailto:hbo@sund.ku.dk)

## Funding information

Carlsbergfondet, Grant/Award Number: CF20-0248; China Scholarship Council, Grant/Award Number: 201907940002; Horizon 2020 Framework Programme, Grant/Award Number: 846827; Novo Nordisk Fonden, Grant/Award Numbers: NNF17OC0028412, NNF19OC0057730

## Abstract

The GPR15 receptor is a G protein-coupled receptor (GPCR), which is activated by an endogenous peptide GPR15L(25–81) and a C-terminal peptide fragment GPR15L(71–81). GPR15 signals through the G<sub>i/o</sub> pathway to decrease intracellular cyclic adenosine 3',5'-monophosphate (cAMP). However, the activation profiles of the GPR15 receptor within G<sub>i/o</sub> subtypes have not been examined. Moreover, whether the receptor can also couple to G<sub>s</sub>, G<sub>q/11</sub> and G<sub>12/13</sub> is unclear. Here, GPR15L(25–81) and GPR15L(71–81) are used as pharmacological tool compounds to delineate the GPR15 receptor-mediated G $\alpha$  protein signalling using a G protein activation assay and second messenger assay conducted on living cells. The results show that the GPR15 receptor preferentially couples to G<sub>i/o</sub> rather than other pathways in both assays. Within the G<sub>i/o</sub> family, the GPR15 receptor activates all the subtypes (G<sub>i1</sub>, G<sub>i2</sub>, G<sub>i3</sub>, G<sub>oA</sub>, G<sub>oB</sub> and G<sub>z</sub>). The E<sub>max</sub> and activation rates of G<sub>i1</sub>, G<sub>i2</sub>, G<sub>i3</sub>, G<sub>oA</sub> and G<sub>oB</sub> are similar, whilst the E<sub>max</sub> of G<sub>z</sub> is smaller and the activation rate is significantly slower. The potencies of both peptides toward each G<sub>i/o</sub> subtype have been determined. Furthermore, the GPR15 receptor signals through G<sub>i/o</sub> to inhibit cAMP accumulation, which could be blocked by the application of the G<sub>i/o</sub> inhibitor pertussis toxin.

## KEYWORDS

BRET, GPR15, G $\alpha$  protein, second messenger, signalling

## 1 | INTRODUCTION

The G protein-coupled receptor 15 (GPR15) is a class A G protein-coupled receptor (GPCR), which was cloned in 1996<sup>1,2</sup> and shown to be a co-receptor for human immunodeficiency virus and simian immunodeficiency

virus infection.<sup>3–5</sup> The GPR15 receptor is widely expressed in the human body, such as the colon,<sup>6</sup> skin<sup>7</sup> and peripheral blood.<sup>8</sup> Published studies have shown that the GPR15 receptor plays an important role in immune disorders such as ulcerative colitis,<sup>9</sup> dermatosis<sup>7,10</sup> and multiple sclerosis.<sup>11</sup> In addition, the

This is an open access article under the terms of the [Creative Commons Attribution-NonCommercial](https://creativecommons.org/licenses/by-nc/4.0/) License, which permits use, distribution and reproduction in any medium, provided the original work is properly cited and is not used for commercial purposes.

© 2022 The Authors. *Basic & Clinical Pharmacology & Toxicology* published by John Wiley & Sons Ltd on behalf of Nordic Association for the Publication of BCPT (former Nordic Pharmacological Society).

GPR15 receptor has been identified as a robust biomarker for tobacco smoking.<sup>12–14</sup> These findings indicate that the GPR15 receptor is a potential therapeutic target for multiple diseases.

The endogenous ligand of the GPR15 receptor, a 57mer peptide termed GPR15L(25–81), has recently been identified by our collaborated laboratory and two other independent research groups.<sup>8,15,16</sup> The GPR15L(25–81) peptide is encoded by chromosome 10 open reading frame 99 (C10orf99) in humans. It is a soluble basic amphiphilic peptide that contains 57-amino acid residues (molecule weight 6.5 KD). It contains two intramolecular disulphide bridges (Cys40 to Cys63 and Cys41 to Cys60) and thus shows resemblance to the structure of chemokine peptides but not to their peptide sequence.<sup>8,15,16</sup> The C-terminal of the GPR15L(25–81) peptide is highly conserved among species and is essential for agonist activity. When deleting the C-terminal region, the peptide is incapable of activating the receptor. However, when progressively deleting the N-terminal amino acids, all truncated constructs (e.g. GPR15L(71–81)) are still capable of activating the GPR15 receptor. The potencies of those truncated variants were positively correlated to their length.<sup>8,15,16</sup> In this study, we used the GPR15L(25–81) and its C-terminal fragment GPR15L(71–81) as pharmacological tool compounds to probe the GPR15 receptor signalling.

There are 17 mammalian  $G\alpha$  proteins<sup>17</sup> that together with  $G\beta$  and  $G\gamma$  subunits form a functional trimeric G protein capable of coupling to GPCRs upon activation by agonists. They have been divided into four classes based on the evolutionary distance, which are  $G_{i/o}$  ( $G_{11}$ ,  $G_{12}$ ,  $G_{13}$ ,  $G_{oA}$ ,  $G_{oB}$ ,  $G_z$ ,  $G_{t1}$ ,  $G_{t2}$ ,  $G_g$ ),  $G_s$  ( $G_s$ ,  $G_{olf}$ ),  $G_{q/11}$  ( $G_q$ ,  $G_{11}$ ,  $G_{14}$ ,  $G_{15/16}$ ) and  $G_{12/13}$  ( $G_{12}$ ,  $G_{13}$ ).<sup>17</sup> The activation of each class of  $G\alpha$  protein leads to distinct downstream signalling pathways. Canonically, the  $G_{i/o}$  inhibits the adenylyl cyclase (AC) and decreases the intracellular cyclic adenosine 3',5'-monophosphate (cAMP) concentration. The  $G_s$  activates the adenylyl cyclase and increases the intracellular cAMP concentration. The  $G_{q/11}$  activates the beta-type phospholipase C and leads to the generation of inositol trisphosphate ( $IP_3$ ) and diacylglycerol.  $G_{12/13}$  activation regulates the small GTPases Rho and leads to c-Jun N-terminal kinase activation.<sup>18</sup>

Our group and others have recently shown that the GPR15 receptor signals via the  $G_{i/o}$  pathway in cAMP second messenger assays.<sup>15,16</sup> However, the coupling “fingerprint” within the  $G_{i/o}$  protein family is unclear. Moreover, whether the GPR15 receptor also couples to the  $G_s$ ,  $G_{q/11}$  and/or  $G_{12/13}$  signalling pathways remains to be determined. In this study, we examined the

coupling selectivity of the GPR15 receptor toward 11  $G\alpha$  proteins representing the four families ( $G_{11}$ ,  $G_{12}$ ,  $G_{13}$ ,  $G_{oA}$ ,  $G_{oB}$ ,  $G_z$ ,  $G_s$ ,  $G_q$ ,  $G_{11}$ ,  $G_{15}$  and  $G_{13}$ ) by conducting the NanoLuc bioluminescence resonance energy transfer (BRET) based G protein activation assay. Wherein the masGRK3ct-Nluc serves as BRET energy donor is anchored on the inside of the cell membrane, and the functional Venus tagged  $G\beta\gamma$  dimer serves as the acceptor is formed based on the bimolecular fluorescence complementation (BiFC) of Venus (155–239)- $G\beta 1$  and Venus (1–155)- $G\gamma 2$ . The BRET will happen when the Venus- $G\beta\gamma$  is released from the heterotrimer and subsequently interacts with the masGRK3ct-Nluc.<sup>19</sup> We tested the downstream signalling of the GPR15 receptor among the  $G_{i/o}$ ,  $G_s$  and  $G_{q/11}$  pathways, by conducting homogeneous time-resolved FRET (HTRF)-based cAMP and  $IP_1$  assays.<sup>20</sup> Moreover, the potencies of the GPR15L(25–81) and GPR15L(71–81) peptides have been determined with both assay formats. The delineation of the GPR15 receptor signalling can contribute to future efforts of drug discovery.

## 2 | MATERIALS AND METHODS

The study was conducted in accordance with the Basic & Clinical Pharmacology & Toxicology policy for experimental and clinical studies.<sup>21</sup>

### 2.1 | Reagents and materials

Dulbecco's Modified Eagle's Medium (DMEM, Cat. No: 12077549), opti-MEM (Cat. No: 51985026), trypsin-ethylenediaminetetraacetic acid (Cat. No: 11590626), penicillin/streptomycin (Cat. No: 11548876), dialyzed foetal bovine serum (FBS, Cat. No: 26400036), Hanks' balanced saline solution without  $Ca^{2+}$  and  $Mg^{2+}$  (Cat. No: 11540476), Dulbecco's phosphate-buffered saline (Cat. No: 14190169), Lipofectamine™ LTX reagent with PLUS™ reagent (Cat. No: 15338100), Lipofectamine 2000 (Cat. No: 11668019), pertussis toxin (PTX, CAS#: 70323-44-3, Cat. No.: PHZ1174), pluronic F-68 non-ionic surfactant (CAS#: 9003-11-6, Cat. No: 24040032), 6-well cell culture plate (Cat. No: 353046) and 10-cm tissue culture dish (Cat. No.: 353003) were obtained from Thermo-Fisher Scientific (Waltham, MA, USA). The 4-(2-hydroxyethyl) piperazine-1-ethanesulfonic acid (HEPES, Cat. No: H4034-500G), antibiotic G418 (CAS#: 108321-42-2, Cat. No: G8168-50ML), bovine serum albumin (BSA, Cat. No: A2153-50G), cell dissociation solution (Cat. No: C5914-100ML), adenylyl cyclase

activator forskolin (FSK, CAS#: 66575-29-9, Cat. No: F6886-10MG), broad-spectrum phosphodiesterase (PDE) inhibitor 3-isobutyl-1-methylxanthine (IBMX, CAS#: 28822-58-4, Cat. No: I5879-250MG), carbamoylcholine chloride (Carbachol, CAS#: 51-83-2, Cat. No: C4382-1G), isoproterenol bitartrate salt (Isoproterenol, CAS#: 54750-10-6, Cat. No: I2760-500MG), glucagon (CAS#: 16941-32-5, Cat. No.: G2044-5MG), lithium chloride (LiCl, CAS#: 7447-41-, Cat. No: 310468-100G-D) and dimethyl sulfoxide (DMSO, CAS#: 67-68-5, Cat. No.: D2650-100ML) were obtained from Sigma Aldrich (St. Louis, MO, USA). The 384-well white opaque microplate for cAMP assay (Cat. No: 784075) was obtained from Greiner. The 384-well white opaque microplate for IP-one assay (Cat. No.: 6007299) and 96-well white opaque (Cat. No.: 6005688) for BRET assay were obtained from PerkinElmer. cAMP-G<sub>s</sub> dynamic kit (Cat. No: 62AM4PEC) and IP-One-Gq kit (Cat. No: 62IPAPEC) were obtained from Cisbio (Codolet, France). Human GPR15L(25–81) peptide sequence: KRRPAKAWSGRRRLCCHRVSPNSTNLKGHHVRLC-KPCKLEPEPRLWVVPALPQV, Cat. No.: 03489) and human GPR15L(71–81) peptide (sequence: LWVVPALPQV, custom made) were obtained from Phoenix Pharmaceuticals. Nano-Glo<sup>®</sup> Luciferase Assay System (Cat. No: N1110) was obtained from Promega. Envision multimode plate reader was obtained from PerkinElmer (Cat. No.: 2104). The multi-mode plate reader POLARstar Omega was from BMG LABTECH.

## 2.2 | Plasmid DNA constructs

Plasmid encoding N-terminal 3xHA tagged GPR15-pcDNA3.1 + (Cat. No: GPR015TN00, human) was obtained from cDNA.org. Plasmids encoding Venus (155–239)-Gβ<sub>1</sub> (human); Venus(1–155)-Gγ<sub>2</sub> (human); mas GRK3ct-Nluc-HA (human); G<sub>i1</sub> (rat); G<sub>i2</sub> (rat); G<sub>i3</sub> (rat); G<sub>oA</sub> (human); G<sub>oB</sub> (human), G<sub>z</sub> (human); G<sub>q</sub> (human); G<sub>11</sub> (human); G<sub>15</sub> (human, also known as human G<sub>16</sub>); G<sub>s</sub> (human); G<sub>13</sub> (human); flag-ric-8A (human); PTX-S1 (human); pcDNA3.1 + (human) were kindly provided by Dr. Kirill Martemyanov, Scripps Research, FL, USA.

## 2.3 | Cell lines and culturing

Cells (passage < 30) were cultured in a 37°C incubator in a humidified 5% CO<sub>2</sub> atmosphere. The culture media for HEK293A cells were DMEM supplemented with 10% dFBS and 100 U/ml penicillin-streptomycin. The

hGPR15-HEK293A (HEK293A cells stably expressing human GPR15 receptor) recombinant cell line was established by selection with G418. The culture media for the stable cell line was DMEM supplemented with 10% dFBS and 500 μg/ml G418. As for the inhibition of G<sub>i/o</sub>, 100 ng/ml of PTX was administered to the cells 24 h before the experiment.

## 2.4 | Transient transfection for BRET G protein activation assay

At 20–24 h before the BRET assay,  $2 \times 10^5$  per well of HEK293A cells were seeded into a 6-well plate. The cells were transfected with 1.26 μg GPR15 receptor DNA, 0.21 μg Venus (155–239)-Gβ<sub>1</sub> DNA, 0.21 μg Venus (1–155)-Gγ<sub>2</sub> DNA, 0.21 μg masGRK3ct-Nluc DNA and an optimized amount of Gα protein DNA (supporting information Table S1). For the successful expression of G<sub>15</sub>, co-transfection with the chaperone Flag-Ric-8A (0.21 μg) is necessary. To avoid the positive BRET signal induced by endogenous G<sub>i/o</sub>, the G proteins from the non-G<sub>i/o</sub> family (i.e. G<sub>q</sub>, G<sub>11</sub>, G<sub>15</sub>, G<sub>s</sub> and G<sub>13</sub>) were co-transfected with 0.21 μg PTX-S1 DNA. The transfection reagents used were Lipofectamine LTX reagent with PLUS reagent and/or Lipofectamine 2000.

## 2.5 | BRET G protein activation assay

The assay step has previously been described by Masuho et al. in detail<sup>22</sup> and is briefly summarized here. *Kinetic assay on LUMIstar plate reader*: 25-μl/well cell suspension (containing 50 000 to 100 000 cells) was added to a white opaque flat-bottom 96-well culture plate. Whereafter 25 μl/well furimazine (1:250 dilution based on the manufacturer's instruction) was added automatically with one of the built-in injectors. The plate was shaken and incubated for 3 min. BRET was then measured by simultaneous measurement of emission at 475 nm (donor) and 535 nm (acceptor). After 5 s of the basal BRET signal measurement, 50 μl/well of the agonist (2 μM GPR15L(25–81) or 20 μM of GPR15L(71–81)) or BRET buffer was added to the wells automatically with another built-in injectors. BRET signals were then measured for 13 s with 0.06 s (G<sub>z</sub>) or 0.02 s (remaining G proteins) intervals. *Endpoint assay on Envision plate reader*: The same procedure as for the LUMIstar was followed except that the agonist was added manually with the multiple channel pipette whereafter the plate was read immediately (practically around 10 s after agonist addition).

## 2.6 | HTRF G<sub>i</sub> cAMP assay

The assays were performed in a 384-well microplate, suspension format as previously described in detail.<sup>23</sup> GPR15L(25–81) and GPR15L(71–81) were threefold diluted in ligand buffer (*Hanks' balanced saline solution supplemented with 20 mM HEPES, 1 mM CaCl<sub>2</sub>, 1 mM MgCl<sub>2</sub>, 3 μM forskolin, and 0.01% freshly added pluronic acid, pH adjusted to 7.4 with NaOH*). The highest concentration (2 × final concentration) of the GPR15L(25–81) and GPR15L(71–81) peptides were 2 μM and 60 μM, respectively. The 5 μl/well of peptide solution was transferred to a 384-well microplate and put aside for later use. HEK293A-GPR15 cells with 80–90% growth confluence were harvested with the non-enzymatic cell dissociation solution. The cells were suspended in 37°C preheated cell suspension buffer (*Hanks' balanced saline solution supplemented with 20 mM HEPES, 1 mM CaCl<sub>2</sub>, 1 mM MgCl<sub>2</sub>, and 100 μM of freshly added IBMX, pH adjusted to 7.4 with NaOH*) with a concentration of 8 × 10<sup>5</sup> cells/ml. Whereafter 5 μl/well (i.e. 4000 cells/well) of cell suspension was added to the 384-well plate. The plate was centrifuged for 10 s at 500 rpm and incubated at room temperature for 30 min. Afterwards, 10 μl/well of freshly made detection solution (*Lysis buffer supplemented with 2.5% cAMP-cryptate and 2.5% anti-cAMP-d2*) was added to the plate in a dim light environment. The plate was incubated for 1 h in the dark at room temperature. Whereafter the plate was read in an Envision plate reader to detect emission at 665 nm and 615 nm simultaneously.

## 2.7 | HTRF G<sub>s</sub> cAMP assay

The assay protocol was performed as described previously.<sup>23</sup> The G<sub>s</sub> cAMP assay procedure was very similar to the G<sub>i</sub> cAMP assay procedure with the only difference being that the ligand buffer used in the G<sub>s</sub> cAMP assay was without forskolin.

## 2.8 | HTRF G<sub>q</sub> IP<sub>1</sub> assay

The assay protocol was performed as described previously.<sup>23</sup> The 5 μl/well of agonists (GPR15L(25–81), GPR15L(71–81), isoproterenol and carbachol) prepared in ligand buffer (*Hanks' balanced saline solution supplemented with 20mM HEPES, 1mM CaCl<sub>2</sub>, 1mM MgCl<sub>2</sub>, and 0.01% freshly added pluronic acid, pH adjusted to 7.4 with NaOH*) with 2 × final concentration was added to the 384-well microplate. The 5 μl of cell suspensions supplemented with 30 mM LiCl and 20 000

HEK293A-GPR15 recombinant cells was added to the agonist-containing plate. The plate was incubated for 30 min at 37°C. Whereafter 10 μl of IP<sub>1</sub> detection solution (IP<sub>1</sub>-cryptate: anti-IP<sub>1</sub>-d2: lysis buffer = 1: 1: 38) was added and followed by incubating the plate in the dark for 1 h at room temperature. The emissions at 665 nm and 615 nm were then recorded simultaneously with the Envision plate reader.

## 2.9 | Data analysis

All statistical analysis was performed with Prism 8 (GraphPad Software, San Diego, CA, USA). Data are presented as the standard error of the mean of at least three independent experiments. Concentration-response curves were fitted with a log (agonist) vs. response-variable slope (four parameters) model to determine the EC<sub>50</sub> value. The kinetic parameter comparisons between the G<sub>z</sub> and other G<sub>i/o</sub> subunits were performed with a one-way analysis of variance test followed by Dunnett's multiple comparison test. The kinetic parameter comparisons between the GPR15L(25–81) and the GPR15L(71–81) were performed with Student's *t* test. The *p* values were indicated by asterisk(s): \*, *p* < 0.05; \*\*, *p* < 0.01; \*\*\*, *p* < 0.001. The HTRF ratio = emission of the d2 at 665 nm/emission of the Eu<sup>3+</sup> cryptate labelled anti-cAMP/IP<sub>1</sub> antibody at 615 nm. cAMP or IP<sub>1</sub> concentrations were calculated from cAMP or IP<sub>1</sub> standard curves. The BRET ratio = emission of Venus at 535 nm/emission of NanoLuc at 475 nm with a 30-nm band path. The BRET ratio amplitude = BRET ratio after agonist or buffer application – BRET ratio before agonist or buffer application. The *E*<sub>max</sub> and the activation rate 1/τ were determined by fitting the kinetic readouts with the one-phase exponential decay equation.

## 3 | RESULTS

### 3.1 | GPR15 receptor preferentially couples to G<sub>i/o</sub> family

We examined the coupling profiles of GPR15 toward 11 representative Gα proteins spanning the four Gα protein families with the NanoLuc BRET G protein activation assay.<sup>19</sup> At 20–24 h before the experiment, we co-transfected the GPR15 receptor, a specific Gα protein and the BRET sensors (Venus(155–239)-Gβ<sub>1</sub>, Venus(1–155)-Gγ<sub>2</sub> and masGRK3ct-Nluc-HA) into wild-type HEK293A cells with optimized DNA amounts (supporting information Table S1). We found that both



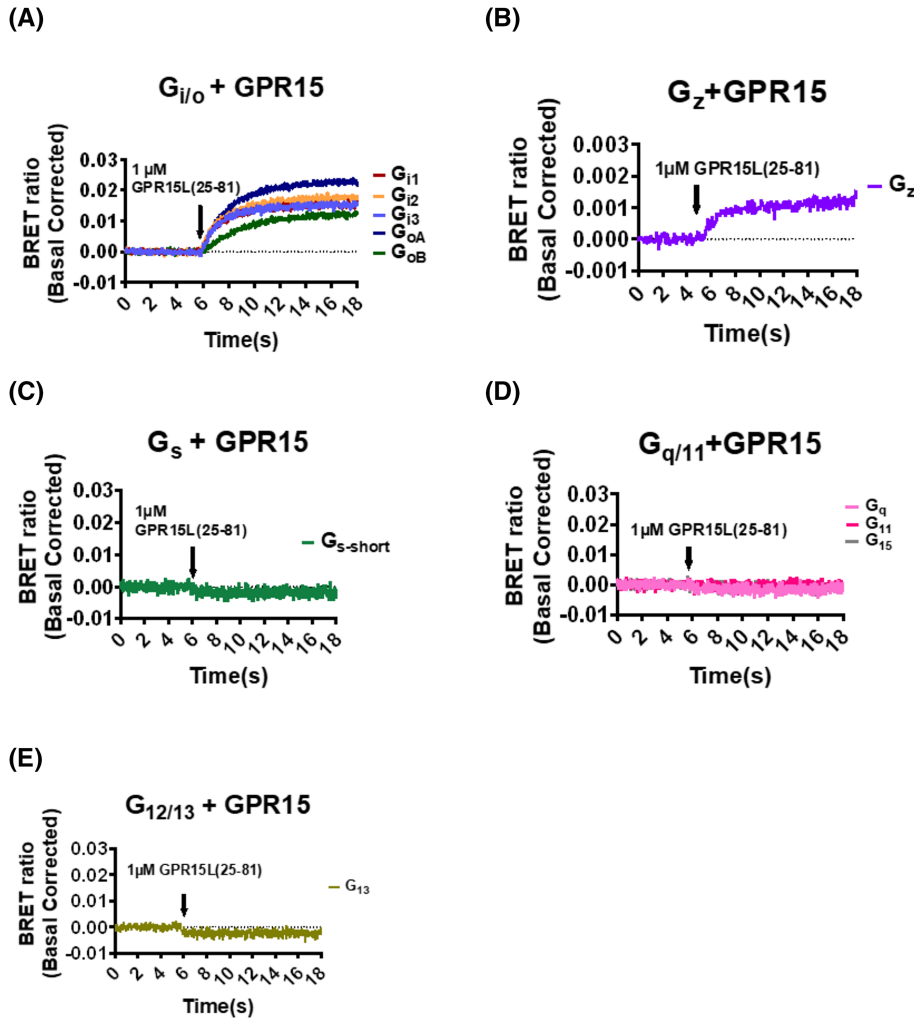


**FIGURE 1** Real-time measurement of G protein coupling profiles of the GPR15 receptor activated by GPR15L (25–81) peptide. (A, B) GPR15,  $G_{\alpha}$ , Venus 155–239  $G\beta 1$ , Venus 1–155  $G\gamma 2$  and masGRK3ct-Nluc-HA transfected HEK293A cells treated with  $1 \mu\text{M}$  of GPR15L(25–81) peptide and activated heterotrimeric  $G_{i/o}$  proteins ( $G_{i1}$ ,  $G_{i2}$ ,  $G_{i3}$ ,  $G_{oA}$ ,  $G_{oB}$  and  $G_z$ ) to release the  $G\beta\gamma$  subunits leading to BRET signal increase. Note the difference in scale of Y axis. (C–E) No response was detected when the cells were treated with  $1 \mu\text{M}$  of GPR15L(25–81) peptide toward G proteins from  $G_s$ ,  $G_{q/11}$  and  $G_{12/13}$  families. The arrow indicates the administration of the agonist. Data plotted as mean  $\pm$  SEM (error bars) of 3–5 grouped independent experiments performed in duplicates. BRET: Bioluminescence resonance energy transfer; SEM: standard error of the mean

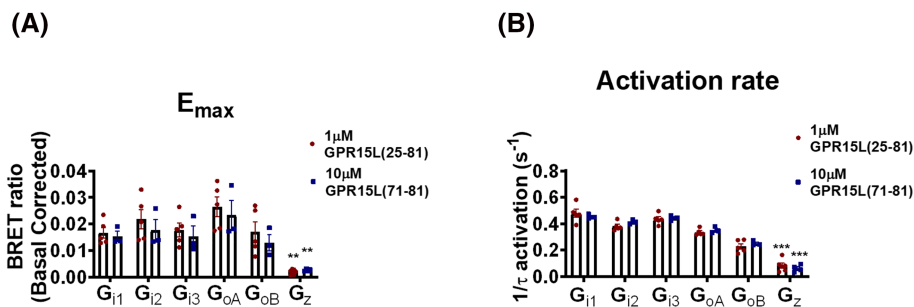


**FIGURE 2** The  $E_{\text{max}}$  and activation rate of the  $G_{i/o}$  activation induced by GPR15L(25–81) and GPR15L(71–81). (A) the  $E_{\text{max}}$  and (B) the activation rates of  $G_{i1}$ ,  $G_{i2}$ ,  $G_{i3}$ ,  $G_{oA}$ ,  $G_{oB}$  and  $G_z$  induced by  $1 \mu\text{M}$  GPR15L(25–81) and  $10 \mu\text{M}$  GPR15L(71–81). The  $E_{\text{max}}$  of  $G_z$  is significantly ( $p < 0.01$ ) smaller than  $G_{i1}$ ,  $G_{i2}$ ,  $G_{i3}$ ,  $G_{oA}$  and  $G_{oB}$ . The activation rate of  $G_z$  is significantly slower than  $G_{i1}$ ,  $G_{i2}$ ,  $G_{i3}$ ,  $G_{oA}$  and  $G_{oB}$  ( $p < 0.001$ ). No significant difference was detected between the GPR15L(25–81) and the GPR15L(71–81) triggered response. The comparisons between the  $G_z$  and other  $G_{i/o}$  subunits were performed with Dunnett's multiple comparison test (\* $p < 0.05$ , \*\* $p < 0.01$ , \*\*\* $p < 0.001$ ). The comparisons between the GPR15L(25–81) and the GPR15L(71–81) were performed with the students  $t$  test. Data plot as mean  $\pm$  SEM (error bars) of 3–5 grouped independent experiments performed in two replicates. BRET: Bioluminescence resonance energy transfer; SEM: standard error of the mean

the GPR15L(25–81) (Figure 1A,B) and the GPR15L(71–81) (supporting information Figure S1A, B) peptides led to effective activation of all the members of the  $G_{i/o}$  family ( $G_{i1}$ ,  $G_{i2}$ ,  $G_{i3}$ ,  $G_{oA}$ ,  $G_{oB}$  and  $G_z$ ). No response to either peptide was detected when the cells were treated with the BRET buffer (supporting information Figure S2), or when cells were only transfected with the  $G\alpha$  protein and the BRET sensors (i.e. no GPR15 receptor present) (supporting information Figure S3A,B). The negative control results demonstrate that the BRET signals in Figure 1A,B, and supporting information Figure 1A, 1B were specifically mediated by the GPR15 receptor and its cognate GPR15L peptides. No response was detected when testing the peptides on cells transfected with the GPR15 receptor and  $G\alpha$  proteins ( $G_s$ ,  $G_q$ ,  $G_{11}$ ,  $G_{15}$  and  $G_{13}$ ) representing the  $G_s$ ,  $G_{q/11}$  and  $G_{12/13}$  families, indicating that the GPR15 receptor does not interact with the  $G_s$ ,  $G_{q/11}$  and  $G_{12/13}$  proteins (Figure 1C,D,E; supporting information Figure S1C, D, E). To ensure assay validity, we included the GCGR that promiscuously couples to all four  $G\alpha$  protein families as a positive control. Our results show that when GCGR was stimulated with 10  $\mu$ M glucagon, GCGR indeed coupled to the  $G_s$ ,  $G_q$ ,  $G_{11}$ ,  $G_{15}$  and  $G_{13}$  (supporting information Figure S4). Taken together, our results show that among the four  $G\alpha$  protein families ( $G_{i/o}$ ,  $G_s$ ,  $G_{q/11}$  and  $G_{12/13}$ ), the GPR15 receptor preferentially couples to the  $G_{i/o}$  signalling pathway and activates all the members of this family effectively.

### 3.2 | The kinetic parameters of the $G_{i/o}$ activation mediated by the GPR15 receptor

Based on data obtained from the kinetic assay, we quantified the  $E_{max}$  and activation rate kinetic parameters. Our results showed that there were no significant ( $p > 0.05$ )

kinetic parameter differences between the GPR15L(25–81) and the GPR15L(71–81) toward all  $G_{i/o}$  proteins (i.e.  $G_{i1}$ ,  $G_{i2}$ ,  $G_{i3}$ ,  $G_{oA}$ ,  $G_{oB}$  and  $G_z$ ) (Figure 2A,B). The activation kinetics among the  $G_{i1}$ ,  $G_{i2}$ ,  $G_{i3}$ ,  $G_{oA}$  and  $G_{oB}$  were quite similar. However, regarding the  $G_z$  activation, when stimulated with the GPR15L(25–81),  $G_z$  produced a much lower  $E_{max}$  and slower activation rate for both versions of peptides (Figure 2A,B). Taken together, the GPR15 receptor showed similar selectivity preference among the  $G_{i1}$ ,  $G_{i2}$ ,  $G_{i3}$ ,  $G_{oA}$  and  $G_{oB}$  with much lower preference for  $G_z$ . Moreover, the GPR15L(25–81) and the

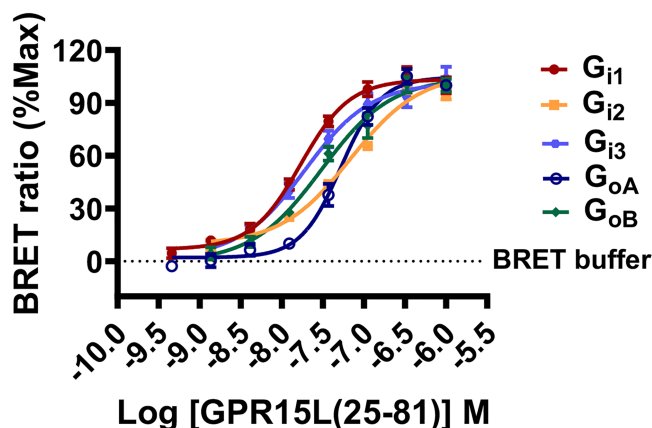


**FIGURE 3** Concentration-response curves of GPR15L(25–81) peptide toward distinct G protein from  $G_{i/o}$  family. Concentration-response curves of the GPR15L(25–81) peptide on  $G_{i1}$ ,  $G_{i2}$ ,  $G_{i3}$ ,  $G_{oA}$  and  $G_{oB}$  proteins were determined by conducting the BRET G protein activation assay on HEK293A cells transiently expressing the GPR15 receptor, the  $G\alpha$  protein and the BRET pair. The  $E_{max}$  of each concentration was buffer corrected and normalized to the max dose-response (100%). Data plotted as mean  $\pm$  SEM (error bars) of 3–5 grouped independent experiments performed in two to three replicates. BRET: Bioluminescence resonance energy transfer; SEM: standard error of the mean.

**TABLE 1**  $pEC_{50}$ ,  $EC_{50}$  and potency ratio summary of the GPR15L(25–81) and GPR15L(71–81) peptide on  $G_{i/o}$  proteins obtained from BRET G protein activation assay and the  $G_i$  cAMP assay. GPR15L(25–81) is more potent than the C-terminal truncated peptide GPR15L(71–81). Potency ratio calculated as  $EC_{50}$  of GPR15L(71–81)/ $EC_{50}$  of GPR15L(25–81). Where a ratio  $>1$  indicates that GPR15L(25–81) is more potent at the individual G protein than GPR15L(71–81), and a larger potency ratio correlates to higher potency differences between the two versions of peptides. Data shown as mean  $\pm$  SEM of 3–5 grouped independent experiments. BRET: Bioluminescence resonance energy transfer; SEM: standard error of the mean

|                              | BRET G protein activation assay |                 |                 |                 |                 | $G_i$ cAMP assay<br>$G_{i/o}$ |
|------------------------------|---------------------------------|-----------------|-----------------|-----------------|-----------------|-------------------------------|
|                              | $G_{i1}$                        | $G_{i2}$        | $G_{i3}$        | $G_{oA}$        | $G_{oB}$        |                               |
| GPR15L(71–81) $pEC_{50}$     | $6.14 \pm 0.05$                 | $5.77 \pm 0.04$ | $6.04 \pm 0.12$ | $5.52 \pm 0.09$ | $5.60 \pm 0.10$ | $6.39 \pm 0.07$               |
| GPR15L(71–81) $EC_{50}$ (nM) | 724                             | 1700            | 912             | 3020            | 2510            | 407                           |
| GPR15L(25–81) $pEC_{50}$     | $7.79 \pm 0.06$                 | $7.14 \pm 0.04$ | $7.69 \pm 0.10$ | $7.28 \pm 0.03$ | $7.54 \pm 0.02$ | $7.96 \pm 0.17$               |
| GPR15L(25–81) $EC_{50}$ (nM) | 16                              | 72              | 20              | 52              | 28              | 10                            |
| Potency ratio                | 45                              | 23              | 45              | 58              | 89              | 40                            |

GPR15L(71–81) induced similar G protein coupling profiles.

### 3.3 | GPR15L peptides activate each $G_{i/o}$ subtype in a concentration-dependent manner

To gain further insight, we determined the potency of the GPR15L(25–81) and its C-terminal fragment GPR15L(71–81) toward activation of the  $G_{i1}$ ,  $G_{i2}$ ,  $G_{i3}$ ,  $G_{oA}$  and  $G_{oB}$  proteins with the BRET G protein activation assay (Table 1). HEK293A cells transiently expressing the GPR15 receptor, the  $G_{i/o}$  protein and the BRET pair were stimulated with increasing concentrations of the GPR15L peptides. The  $E_{max}$  of each concentration was recorded to determine the concentration-response curve. Our results showed that both GPR15L(25–81) (Figure 3) and GPR15L(71–81) (supporting information Figure S5) activated each  $G_{i/o}$  protein in a concentration-dependent manner. The GPR15L(25–81) was more potent than the GPR15L

(71–81) on each  $G_{i/o}$  protein. The potency ratio (i.e.  $EC_{50}$  of GPR15L(71–81)/ $EC_{50}$  of GPR15L(25–81)) was 45, 23, 45, 58 and 89 toward  $G_{i1}$ ,  $G_{i2}$ ,  $G_{i3}$ ,  $G_{oA}$  and  $G_{oB}$ , respectively (Table 1).

### 3.4 | GPR15 receptor signals through $G_{i/o}$ rather than $G_s$ and $G_{q/11}$ in the downstream signalling pathway

The results described above were obtained from the BRET G protein activation assay, which reflects the proximity of the GPCR and G protein, upstream of the signal cascade. Next, we also investigated the downstream signalling pathway by measuring second messenger molecules cAMP and  $IP_1$ . We measured cAMP accumulation in  $G_{i/o}$  and  $G_s$  mode by including/excluding the adenylate cyclase activator forskolin, respectively. The pan-phosphodiesterase inhibitor IBMX was applied to prevent the cAMP degradation in the

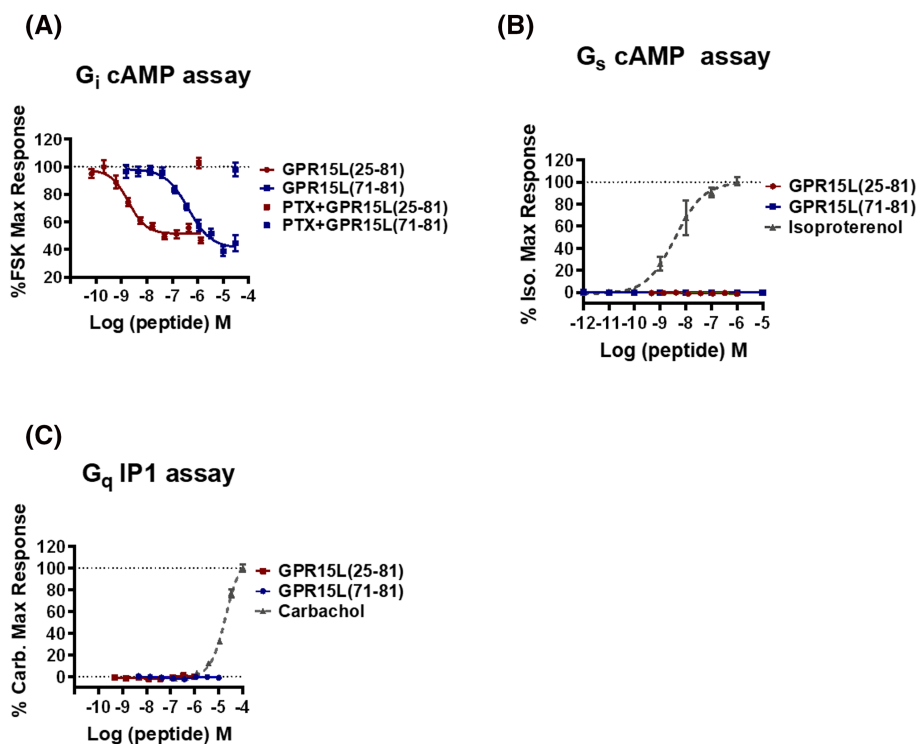


**FIGURE 4** Concentration-response curves of the GPR15L peptides in three HTRF based assays of  $G_i$ ,  $G_o$  and  $G_q$  downstream pathways. (A) Concentration-response curves of full-length GPR15L(25–81) and C-terminal peptide GPR15L(71–81) with a  $G_i$  cAMP assay conducted on the HEK293A-GPR15 recombinant cells. The activation effect of the GPR15L peptides could be blocked by the  $G_{i/o}$  inhibitor PTX. (B) Concentration-response curves of the GPR15L peptides in the  $G_s$  cAMP assay. The endogenously expressed  $\beta_2$ -adrenergic receptor and its agonist isoproterenol was used as positive control. (C) Concentration-response curves of the GPR15L peptides in the  $G_q$   $IP_1$  assay. The endogenously expressed muscarinic acetylcholine receptor ( $mAChR1$ ,  $mAChR3$  and  $mAChR5$ ) and its agonist carbachol was used as positive control. Data were buffer corrected and then normalized to the maximal response of FSK (forskolin), isoproterenol and carbachol, respectively. Data plotted as mean  $\pm$  S.E.M. (error bars) of 3–5 grouped independent experiments performed in three replicates. HTRF: homogenous time-resolved Förster resonance energy transfer; PTX: pertussis toxin; FSK: forskolin; Iso: isoproterenol; carb.: carbachol; SEM: standard error of the mean

cAMP assay. The  $G_q$  pathway was assessed by measurement of  $IP_1$  accumulation in the presence of LiCl to prevent further breakdown to inositol monophosphate. All three pathways were endpoint assays based on HTRF technology.<sup>23,24</sup>

In the  $G_i$  cAMP assay, both GPR15L peptides led to decreased intracellular cAMP concentrations in a concentration-dependent manner (Figure 4A). The GPR15L(25–81) peptide was 40-fold more potent than its C-terminal fragment GPR15L(71–81) (Table 1). Moreover, the inhibition could be eliminated by the  $G_{i/o}$  inhibitor PTX (Figure 4A) demonstrating that the negative regulation of cAMP production was mediated by  $G_{i/o}$  proteins.

In the  $G_s$  cAMP assay, no cAMP response was detected by either GPR15L peptide. To ensure assay validity, the  $G_s$  coupled  $\beta_2$ -adrenergic receptor, which is endogenously expressed in the parental HEK293A cells, was used as a positive control.<sup>25</sup> We detected a robust cAMP level increase when stimulating with the cells with the  $\beta_2$ -adrenergic receptor agonist isoproterenol (Figure 4B).

In the  $G_q$   $IP_1$  assay, no  $IP_1$  response was detected by either GPR15L peptide. To ensure assay validity, we used endogenously expressed  $G_q$  coupled muscarinic acetylcholine receptors as a positive control. We detected a robust  $IP_1$  level increase when stimulating the HEK293A cells with the muscarinic receptor agonist carbachol (Figure 4C).

## 4 | DISCUSSION

In this study, by combining the upstream G protein activation assay and the canonical downstream assays, we demonstrated that, among the four G protein families ( $G_{i/o}$ ,  $G_{s/olf}$ ,  $G_{q/11}$  and  $G_{12/13}$ ), the GPR15 receptor preferentially couples to the  $G_{i/o}$  family. Moreover, the GPR15 receptor couples to all members of the  $G_{i/o}$  protein subtypes ( $G_{i1}$ ,  $G_{i2}$ ,  $G_{i3}$ ,  $G_{oA}$ ,  $G_{oB}$  and  $G_z$ ) and with the least preference to the  $G_z$  subtype. The endogenous peptide ligand GPR15L(25–81) is more potent than its C-terminal peptide GPR15L(71–81). Except for this, both versions of peptides display the same overall signalling profiles.

We thus validate former studies which have shown that the GPR15 receptor signals through  $G_{i/o}$ .<sup>8,15,16</sup> However, those results were all obtained from the distal part of the signal cascades, where accuracy may be affected due to potential signalling crosstalk. To gain further insight, we conducted a BRET-based G protein activation assay, which enables the direct examination of the GPR15 receptor-mediated  $G\alpha$  protein activation. Our results show that the GPR15 receptor coupling profiles

are highly consistent between the upstream and downstream assays. Recently, it has been shown that some GPCRs paradoxically recruit/activate G proteins without activating the downstream signalling pathways.<sup>26,27</sup> Our results clearly show that this behaviour is not observed for GPR15.

Suply et al. observed calcium signalling when the GPR15 receptor co-expressed with  $G_{16}$  in CHO-K1 cells was stimulated by GPR15L peptides,<sup>15</sup> which suggests that GPR15 can activate the promiscuous  $G_{16}$  protein and putatively also other members of the  $G_{q/11}$  family. However, we did not detect activation of  $G_q$ ,  $G_{11}$  or  $G_{15}$ , or  $IP_1$  accumulation in HEK293A cells.<sup>28</sup> This discrepancy could either be caused by differences in cell background, in assay sensitivity, or in assay formats.

Our concentration-response experiments show that the endogenous peptide ligand GPR15L(25–81) ( $EC_{50} = 10$  nM) is 40-fold more potent than its C-terminal peptide GPR15L(71–81) ( $EC_{50} = 407$  nM) in the  $G_i$  cAMP assay. The GPR15L(25–81) is also more potent (23- to 89-fold) than GPR15L(71–81) in the BRET  $G_{i/o}$  protein activation assay. This potency difference agrees well with our previous findings. Wherein the C-terminal fragments of GPR15L(25–81), peptides were tested with the same  $G_i$  cAMP assay as we did here, but using T-REX 293 cells which need doxycycline to induce GPR15 expression, and where we found that the ability of GPR15L peptides to activate GPR15 are positively correlating to their lengths.<sup>16</sup> We were incapable of determining concentration-response curves for  $G_z$  in the BRET G protein activation assay due to the very small  $E_{max}$  of  $G_z$ . To boost the signal, co-transfection with regulators of G protein signalling proteins may be necessary.

In conclusion, our results demonstrate that the GPR15 receptor shows a high preference for  $G_{i/o}$  signalling when expressed in HEK293A. So far, no such studies have been performed on cells with native GPR15 expressions such as the colon colorectal adenocarcinoma cell lines SW48 and HT29, or some lymphoblast cells such as PM1, Hut78 and NC37,<sup>5,29,30</sup> which will be important in future studies to determine if the signalling profile in recombinant systems is translatable to the ex vivo situation. To this end, it will also be important to develop better tool ligands such as the first antagonists and small molecule ligands as the current pharmacological toolbox is very limited and not suitable for in vivo studies.

## ACKNOWLEDGEMENTS

This project was funded by the China Scholarship Council (Grant #201907940002 to Y.D.), the Novo Nordisk Foundation (Grants NNF17OC0028412 and NNF19OC0057730 to H.B.-O.), the Carlsberg Foundation



(Grant CF20-0248 to H.B.-O.) and the European Union's Horizon2020 research and innovation program under the Marie Skłodowska-Curie grant agreement No 846827 (E.V.M.)


## CONFLICT OF INTEREST

The authors declared that there are no conflicts of interest in this study.

## ORCID

Yufang Deng  <https://orcid.org/0000-0002-0104-1344>

Ee Von Moo  <https://orcid.org/0000-0003-2629-9779>

Claudia Victoria Pérez Almería  <https://orcid.org/0000-0002-7312-8529>

Patrick R. Gentry  <https://orcid.org/0000-0003-0670-6648>

Jesper M. Mathiesen  <https://orcid.org/0000-0003-4251-4416>

Hans Bräuner-Osborne  <https://orcid.org/0000-0001-9495-7388>

## REFERENCES

- Heiber M, Marchese A, Nguyen T, Heng HH, George SR, O'Dowd BF. A novel human gene encoding a G-protein-coupled receptor (GPR15) is located on chromosome 3. *Genomics*. 1996;32(3):462-465. doi:10.1006/geno.1996.0143
- Prétet JL, Brussel A, Guillet JG, Butor C. Two alleles for rhesus macaque GPR15 (BOB). *AIDS Res Hum Retroviruses*. 1999; 15(10):945-947. doi:10.1089/088922299310665
- Blaak H, Boers PH, Gruters RA, Schuitemaker H, van der Ende ME, CCR5 OAD. GPR15, and CXCR6 are major coreceptors of human immunodeficiency virus type 2 variants isolated from individuals with and without plasma viremia. *J Virol*. 2005;79(3):1686-1700. doi:10.1128/JVI.79.3.1686-1700.2005
- Kiene M, Marzi A, Urbanczyk A, et al. The role of the alternative coreceptor GPR15 in SIV tropism for human cells. *Virology*. 2012;433(1):73-84. doi:10.1016/j.virol.2012.07.012
- Clayton F, Kotler DP, Kuwada SK, et al. Gp120-induced Bob/GPR15 activation: a possible cause of human immunodeficiency virus enteropathy. *Am J Pathol*. 2001;159(5):1933-1939. doi:10.1016/S0002-9440(10)63040-4
- Nguyen LP, Pan J, Dinh TT, et al. Role and species-specific expression of colon T cell homing receptor GPR15 in colitis. *Nat Immunol*. 2015;16(2):207-213. doi:10.1038/ni.3079
- Lahl K, Sweere J, Pan J, Butcher E. Orphan chemoattractant receptor GPR15 mediates dendritic epidermal T-cell recruitment to the skin. *Eur J Immunol*. 2014;44(9):2577-2581. doi:10.1002/eji.201444628
- Ocón B, Pan J, Dinh TT, et al. A mucosal and cutaneous chemokine ligand for the lymphocyte chemoattractant receptor GPR15. *Front Immunol*. 2017;8:1111. doi:10.3389/fimmu.2017.01111
- Adamczyk A, Gageik D, Frede A, et al. Differential expression of GPR15 on T cells during ulcerative colitis. *JCI Insight*. 2017; 2(8):e90585. doi:10.1172/jci.insight.90585
- Jegodzinski L, Sezin T, Loser K, Mousavi S, Zillikens D, Sadik CD. The G protein-coupled receptor (GPR) 15 counteracts antibody-mediated skin inflammation. *Front Immunol*. 2020;11:1858. Published 2020 Aug 14 doi:10.3389/fimmu.2020.01858
- Ammitzbøll C, von Essen MR, Börnsen L, et al. GPR15+ T cells are Th17 like, increased in smokers and associated with multiple sclerosis. *J Autoimmun*. 2019;97:114-121. doi:10.1016/j.jaut.2018.09.005
- Köks G, Udelepp ML, Limbach M, Peterson P, Reimann E, Köks S. Smoking-induced expression of the GPR15 gene indicates its potential role in chronic inflammatory pathologies. *Am J Pathol*. 2015;185(11):2898-2906. doi:10.1016/j.ajpath.2015.07.006
- Bauer M, Fink B, Seyfarth HJ, Wirtz H, Frille A. Tobacco-smoking induced GPR15-expressing T cells in blood do not indicate pulmonary damage. *BMC Pulm Med*. 2017;17(1):159. doi:10.1186/s12890-017-0509-0
- Köks S, Köks G. Activation of GPR15 and its involvement in the biological effects of smoking. *Exp Biol Med (Maywood)*. 2017;242(11):1207-1212. doi:10.1177/1535370217703977
- Suply T, Hannedouche S, Carte N, et al. A natural ligand for the orphan receptor GPR15 modulates lymphocyte recruitment to epithelia. *Sci Signal*. 2017;10(496):eaal0180. doi:10.1126/scisignal.aal0180
- Foster SR, Hauser AS, Vedel L, et al. Discovery of human signaling systems: Pairing peptides to G protein-coupled receptors. *Cell*. 2019;179(4):895, e21-908. doi:10.1016/j.cell.2019.10.010
- Syrovatkina V, Alegre KO, Dey R, Huang XY. Regulation, signaling, and physiological functions of G-proteins. *J Mol Biol*. 2016;428(19):3850-3868. doi:10.1016/j.jmb.2016.08.002
- Neves SR, Ram PT, Iyengar R. G protein pathways. *Science*. 2002;296(5573):1636-1639. doi:10.1126/science.1071550
- Masuh I, Ostrovskaya O, Kramer GM, Jones CD, Xie K, Martemyanov KA. Distinct profiles of functional discrimination among G proteins determine the actions of G protein-coupled receptors. *Sci Signal*. 2015;8(405):ra123. doi:10.1126/scisignal.aab4068
- Lohse MJ, Nuber S, Hoffmann C. Fluorescence/bioluminescence resonance energy transfer techniques to study G-protein-coupled receptor activation and signaling. *Pharmacol Rev*. 2012;64(2):299-336. doi:10.1124/pr.110.004309
- Tveden-Nyborg P, Bergmann TK, Jessen N, Simonsen U, Lykkesfeldt J. BCPT policy for experimental and clinical studies. *Basic Clin Pharmacol Toxicol*. 2021;128(1):4-8. doi:10.1111/bcpt.13492
- Masuh I, Martemyanov KA, Lambert NA. Monitoring G protein activation in cells with BRET. *Methods Mol Biol*. 2015; 1335:107-113. doi:10.1007/978-1-4939-2914-6\_8
- Nørskov-Lauritsen L, Thomsen AR, Bräuner-Osborne H. G protein-coupled receptor signaling analysis using homogenous time-resolved Förster resonance energy transfer (HTRF®) technology. *Int J Mol Sci*. 2014;15(2):2554-2572. doi:10.3390/ijms15022554
- Degorce F, Card A, Soh S, Trinquet E, Knapik GP, Xie B. HTRF: a technology tailored for drug discovery—a review of theoretical aspects and recent applications. *Curr Chem Genomics*. 2009;3(1):22-32. doi:10.2174/1875397300903010022

25. Schmitt JM, Stork PJ. beta 2-adrenergic receptor activates extracellular signal-regulated kinases (ERKs) via the small G protein rap1 and the serine/threonine kinase B-Raf. *J Biol Chem.* 2000;275(33):25342-25350. doi:[10.1074/jbc.M003213200](https://doi.org/10.1074/jbc.M003213200)
26. Okashah N, Wright SC, Kawakami K, et al. Agonist-induced formation of unproductive receptor-G12 complexes. *Proc Natl Acad Sci U S A.* 2020;117(35):21723-21730. doi:[10.1073/pnas.2003787117](https://doi.org/10.1073/pnas.2003787117)
27. Stoveken HM, Zucca S, Masuho I, Grill B, Martemyanov KA. The orphan receptor GPR139 signals via Gq/11 to oppose opioid effects. *J Biol Chem.* 2020;295(31):10822-10830. doi:[10.1074/jbc.AC120.014770](https://doi.org/10.1074/jbc.AC120.014770)
28. Atwood BK, Lopez J, Wager-Miller J, Mackie K, Straiker A. Expression of G protein-coupled receptors and related proteins in HEK293, AtT20, BV2, and N18 cell lines as revealed by microarray analysis. *BMC Genomics.* 2011;12(1):14. doi:[10.1186/1471-2164-12-14](https://doi.org/10.1186/1471-2164-12-14)
29. Bassilana F, Baumgarten BU, Carte NMT, et al. Organic Compounds. US Patent 10,203,327 B2. Feb. 12, 2019.
30. Okamoto Y, Shikano S. Differential phosphorylation signals control endocytosis of GPR15. *Mol Biol Cell.* 2017;28(17):2267-2281. doi:[10.1091/mbc.E16-09-0627](https://doi.org/10.1091/mbc.E16-09-0627)

### SUPPORTING INFORMATION

Additional supporting information may be found in the online version of the article at the publisher's website.

**How to cite this article:** Deng Y, Moo EV, Almería CVP, et al. Delineation of the GPR15 receptor-mediated G $\alpha$  protein signalling profile in recombinant mammalian cells. *Basic Clin Pharmacol Toxicol.* 2022;131(2):104-113. doi:[10.1111/bcpt.13738](https://doi.org/10.1111/bcpt.13738)